Receptor Ca Current and Ca-gated K Current in Tonic Electroreceptors of the Marine Catfish *Plotosus*

YOSHIKO SUGAWARA and SHOSAKU OBARA

From the Department of Physiology, Teikyo University School of Medicine, Itabashi-ku, Tokyo 173, Japan

ABSTRACT The tonic electroreceptors of the marine catfish *Plotosus* consist of a cluster of ampullae of sensory epithelia, each of which is an isolated receptor unit that is attached to the distant skin with only a long duct. The single-cell layered sensory epithelium has pear-shaped receptor cells interspersed with thin processes of supporting cells. The apical border of the receptor cells is joined to the supporting cells with junctional complexes. Single ampullae were excised and electrically isolated by an air gap. Receptor responses were recorded as epithelial current under voltage clamp, and postsynaptic potentials (PSP) were recorded externally from the afferent nerve in the presence of tetrodotoxin. The ampulla showed a DC potential of -19.2 ± 6.5 mV (mean ± SD, $n = 18$), and an input resistance of 697 ± 263 KΩ ($n = 21$). Positive voltage steps evoked inward currents with two peaks and a positive dip, associated with PSPs. The apical membrane proved to be inactive. The inward current was ascribed to Ca current, and the positive dip to Ca-gated transient K current, bot in the basal membrane of receptor cells. The Ca channels proved to have ionic selectivity in the order of $Sr^{2+} > Ca^{2+} > Ba^{2+}$, and presumably they also passed outward current nonselectively. Double-pulse experiments further revealed a current-dependent inactivation for a part of the Ca current.

INTRODUCTION

The responses of the sensory receptor are generally dependent on monovalent cations such as Na^+ and K^+. The contribution of Ca^{2+}, in addition to K^+, to the mechanoreceptive response was first reported in *Paramecium* (Naitoh and Eckert, 1969). The Ca-dependent receptor potential has since been shown in a number of electroreceptors of fish (Zipser and Bennett, 1973; Akutsu and Obara, 1974; Clusin and Bennet, 1977*a*, *b*, 1979*a*, *b*; Zakon, 1984). Ca^{2+} is further involved in various aspects of receptor operation, as shown in the lateral-line organ (Sand, 1975), in the retinal rod (Fain, et al., 1977) and in the barnacle photoreceptor (Ross and Stuart, 1978). Although not directly involved for receptor electrogenesis, a minimum amount of Ca^{2+} is required for mechanotransduction in the vestibular hair cells of

Address reprint requests to Dr. Yoshiko Sugawara, Department of Physiology, Teikyo University School of Medicine, Kaga 2-11-1, Itabashi-ku, Tokyo 173, Japan.

J. GEN. PHYSIOL. © The Rockefeller University Press · 0022-1295/89/02/0343/22 $2.00
Volume 93 February 1989 343–364

chick (Ohmori, 1984*b*). In several electroreceptors and in some hair cells, Ca-gated K current has been shown to induce oscillatory receptor responses, which seem to serve for sensory adaptation or for frequency tuning (Clusin and Bennett, 1979*b*; Zakon, 1984; Hudspeth, 1985). Thus, Ca^{2+} plays multiple roles in such second-order sensory organs, not only in the process of transmitter release but also in the transduction process.

The ampullary electroreceptor of *Plotosus* provides useful preparation for analysis of receptor operation. Each ampulla consists of a sac of the sensory epithelium connected to the skin only by a long duct, and hence is readily excised as an independent receptor unit. The receptor activity can be recorded from inside the ampulla, and the postsynaptic activity from the nerve, both as mass responses. The ampullary response in situ is small and graded since low axial impedance of the duct electrically shunts the ampulla (Obara, 1974). With the shunt removed or the sensory epithelium electrically isolated, however, the response can be studied under current- or voltage-clamp conditions (Sugawara and Obara, 1979).

In the present study, the receptor activity is recorded as epithelial currents under voltage-clamp. Results indicate that the receptor current is carried through Ca channel and Ca-gated K channel in the basal membrane of the receptor cells. The receptor Ca current shows several properties similar to other Ca currents. Preliminary reports have appeared elsewhere (Sugawara and Kanaseki, 1976; Sugawara and Obara, 1979).

METHODS

Materials

The marine catfish *Plotosus anguillaris* (Lacépède) were collected by local fishermen, and kept in laboratory aquaria until use. All experiments were carried out on isolated ampullary electroreceptors. The fish was initially anesthetized by MS 222, immobilized by curare, and maintained by perfusing sea water through the gills. The dorsal ampullae were exposed by opening the thick connective capsule, and by removing a mass of fatty tissue that embedded the ampullae. The room temperature was kept at 20–23°C.

Anatomical Methods

The dorsal group of ampullae was excised and immediately immersed in the primary fixative, 1% paraformaldehyde and 0.7% glutaraldehyde in 0.1 M/liter phosphate and *s*-collidine buffer at pH 7.4 (modified Karnovsky's method). The tissue was trimmed into small pieces, and left in the primary fixative for 1–2 h at room temperature. After a rinse with phosphate buffer in distilled water, the tissue was postfixed with 1% osmium tetroxide in 0.028 M acetate-veronal buffer (Palade's solution) for 1–2 h at 4°C. The tissue was stained *en bloc* with 0.5% uranyl acetate in Millonig's acetate-veronal buffer at pH 5 for 1–2 h at room temperature, dehydrated in a graded series of ethanol, and then embedded in Epon 812 by the standard method. Thin sections were cut by a diamond knife on a Porter-Blum ultramicrotome (MT-2B; Sorvall, New Haven, CT). The sections were stained with Millonig's lead acetate. Observations were made using the electron miscroscopes HU-12AS (Hitachi, Tokyo, Japan) and JEM 200A (Nihon Densi, Tokyo, Japan).

Physiological Methods

A given ampulla in the supraorbital group was dissected out, with its 1–2-cm-long duct and a short stretch of the nerve. The excised ampulla was placed in a small chamber with two saline pools that were separated by a 2-mm air gap (Fig. 1 *B*). The pool with the ampulla was grounded by a calomel electrode via a KCl-agar bridge and was continuously perfused with saline. The other pool contained the cut end of the duct, which was introduced into a capillary equipped with a pair of Ag-AgCl wire electrodes for stimulation and monitoring. The ampullary responses were recorded as potential changes across the sensory epithelium, differentially between two microelectrodes, one of which was inside the duct near the ampulla (Fig. 1 *B*, V) and the other was just outside (not shown). The glass microelectrodes were filled with

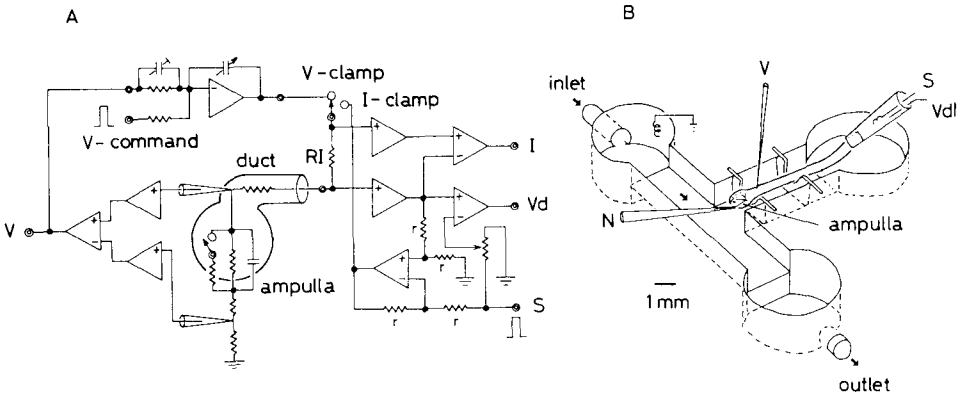

FIGURE 1. Experimental set-up with the isolated *Plotosus* electroreceptor. *A* shows the circuit with a mode switch for *V*-clamp and *I*-clamp. The potential in the ampulla (*V*) was recorded differentially across the sensory epithelium. In *I*-clamp, the potential in the duct (V_d) was recorded by a suction electrode, as shown in *B*. After the *V* and V_d became identical, the mode switch was changed to *V*-clamp. In *V*-clamp, the receptor current (*I*) was measured as a voltage drop across *RI*. *B* shows the experimental chamber with two saline pools connected by a shallow trough. The ampulla was placed in one pool with an inlet and an outlet for solution exchange. The duct bridged a 2-mm air gap in the trough to the other pool with electrodes for stimulation (*S*) and recording (*Vd*). The afferent nerve activity (*N*) was recorded by a thin suction electrode. The solution exchange was complete in 1 min at a flow rate of 1.5 ml/min.

2.5 M/liter KCl, and had a resistance of 7–10 MΩ. The afferent nerve activity was recorded as PSPs by a thin suction electrode (*N*).

Measurement of the Epithelial Current

Fig. 1 *A* shows the experimental arrangements for current- and voltage-clamp (*I*-clamp and *V*-clamp). The response in the ampulla was first compared with that in the duct under *I*-clamp. Since the outside of the duct was desiccated in the air gap, the response size at the two recording sites became identical. This was taken to indicate that there was no axial current in the duct, that the ampullary response was electrically isolated, and that the epithelium was spatially clamped (Akutsu and Obara, 1974). After this condition was obtained, the mode switch was changed to *V*-clamp. Prolonged exposure of the duct in the air gap often caused

an increase in the axial resistance, owing to excessive desiccation, which resulted in *V*-clamp failure because of a series resistance between the microelectrode tip and the epithelium. A floating Ir-Pt wire (25 μm in diameter), left inserted in the duct, retarded such uncontrollable changes, and stable *V*-clamp conditions were maintained over 1 h. The clamp failure was indicated by a prolonged capacitative surge and an anomalous current pattern such as inverted voltage responses. The experiment was discontinued upon these criteria.

The epithelial current was conventionally recorded as in Fig. 1 *A*, with a high voltage-output clamp amplifier (CEZ-1100, Nihonkoden, Tokyo, Japan). As the duct provided a low-resistance access to the ampullary lumen, the voltage responses upon small command steps could reach 90% of the steady value within 300 μs. The epithelial current, however, took ~2 ms to settle owing to a complex capacitative property of the epithelium.

Solutions

Standard saline contained (in millimolar): 190 NaCl, 4 KCl, 3 $CaCl_2$, 1.5 $MgCl_2$, and 8.5 HEPES buffer adjusted to pH 7.2–7.4. In most of the later experiments for ionic substitution, the saline was slightly modified (control saline): 190 NaCl, 3 $CaCl_2$, 1.5 $MgCl_2$, 10 glucose, and 8.5 HEPES. Omission of KCl had little effect on the response pattern (Akutsu and Obara, 1974), while simplifying substitution. Addition of glucose proved to definitely improve the survival time of the preparation. The Ca concentration was modified by isosmotic substitution with $CaCl_2$ for NaCl. Ba- or Sr-saline was prepared by addition of 1 M/liter stock solutions of $BaCl_2$ or $SrCl_2$ to Ca-free saline. Other divalent cations, such as Co^{2+}, Mn^{2+} or Mg^{2+}, were simply added to the control saline. Ionic blockers, such as verapamil, tetrodotoxin (TTX), or 4-aminopyridine (4-AP), were also similarly added to the control saline. Tetraethylammonium chloride (TEA) was isosmotically substituted for NaCl.

RESULTS

Morphology

The general organization of the *Plotosus* receptor has been described previously (Friedrich-Freksa, 1930; Lekander, 1949; Obara, 1974). Briefly, a cluster of ~80 ampullae is embedded in a mass of fatty tissue under a thick capsule supplied with fine blood capillaries. Each ampulla is a sac of sensory epithelium of 379 ± 72.0 μm in diameter (mean ±SD, $n = 30$), and is open to the outside over the skin through a transparent tube a few centimeters long. This tube will be called an ampullary duct, to distinguish it from thicker-walled and opaque canal of the lateral-line canal

FIGURE 2. (*Opposite*) Fine structure of the sensory epithelium of the *Plotosus* receptor. *A* shows the pear-shaped receptor cells (*RC*) interspersed with thin processes of the supporting cells (*SC*). Basal to them are the basement membrane and thick layers of collagen fibers (*Co*). The receptor cells bear microvilli on the apical face, and afferent synapses (arrow) on the basal face. In *B*, a myelinated afferent nerve fiber (*N*) sheds the myelin sheath upon penetrating the basement membrane, and makes synaptic contacts (arrow) on the receptor cell. *C* shows the microvilli. The cytoplasm of the receptor cell has numerous vesicles and smooth endoplasmic reticuli, and the apical process of the supporting cell has a cluster of larger vesicles. *D* shows the nerve terminal filled with mitochondria (*Mit*) and glycogen particles (*G*), and dense bodies (*DB*) are in the receptor cell. In *E*, the dense bodies surrounded by synaptic vesicles are homogeneous near the synaptic area, but loosely packed in opposite parts. Calibration bars represent 5 μm in *A* and *B*, and 1 μm in *C*, *D*, and *E*.

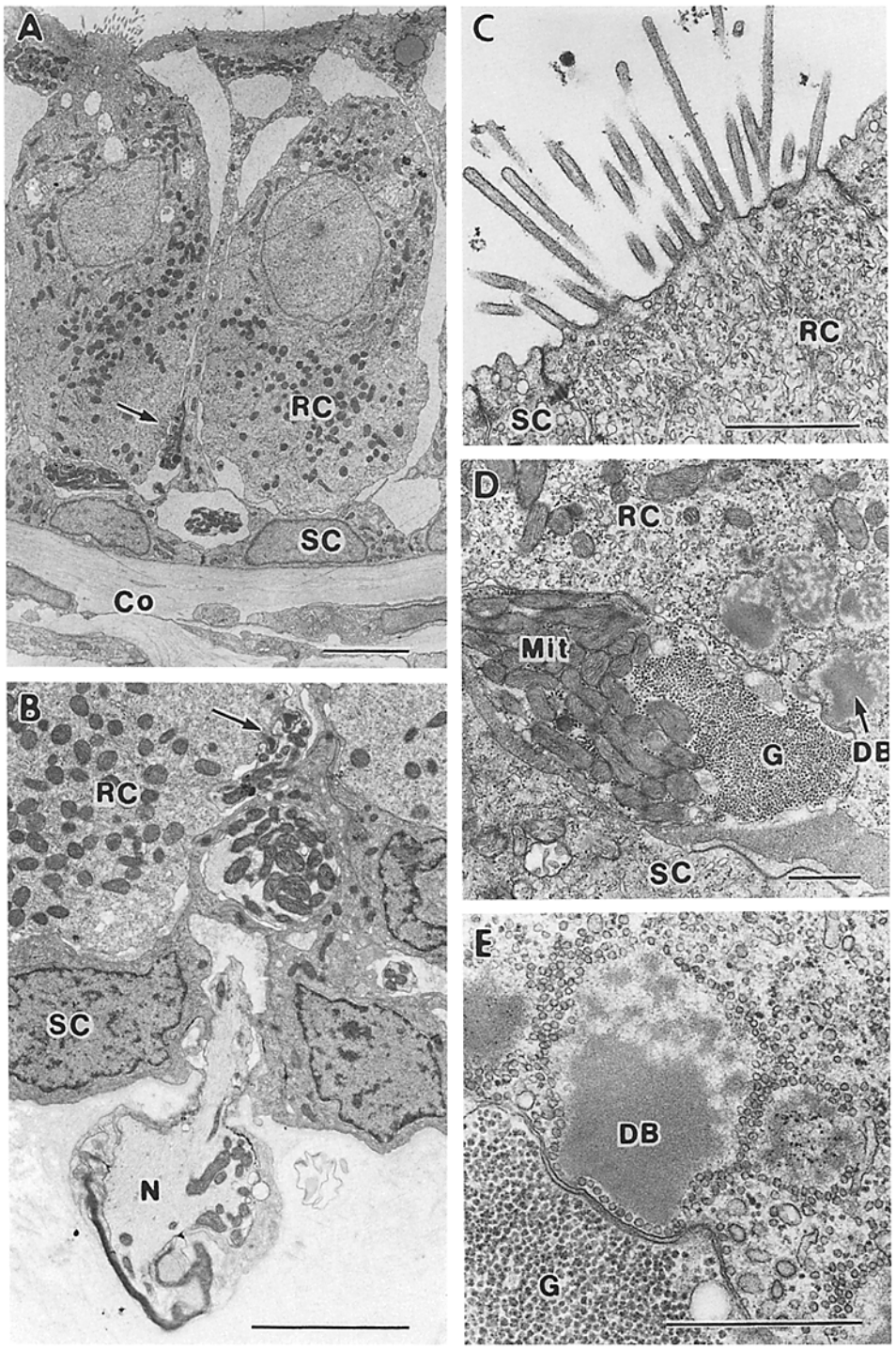

FIGURE 2.

organ, even though they overlap in places under the skin. The duct is 166.8 ± 42.8 μm in diameter near the ampulla, but it can become about twice as large outside the capsule. The ampulla and the duct are filled with K-rich jelly so that conductivity is high, similar to the sea water (Okitsu et al., 1978). Each ampulla is supplied with 6–8 myelinated afferent fibers from the anterior lateral-line nerve. No efferent innervation has been observed.

The epithelium is single-cell layered and 20–30 μm thick after fixation (Fig 2 *A*). The receptor cells form tight junctional complexes (*A* and *C*) around the apical border with the interspersed thin cytoplasmic processes of the supporting cells, the pericaryon of which are found below the receptor cells. This general organization is similar to that of other ampullary receptors (Waltman, 1966; Lissmann and Mullinger, 1968). The spherical epithelium is surrounded by a basement membrane, and further by closely packed connective tissue layers of about the same thickness.

The receptor cells are pear-shaped, 15–25 μm in height and 8–15 μm in diameter. Thus, there would be 700–1,000 receptor cells per ampulla. The apical face over the junctional complex bears sparse microvilli ~2 μm long and 100 nm in diameter (Fig. 2 *C*). No kinocilium or structures such as basal body are found, unlike those in the skate receptors (Waltman, 1966). The lateral surface is devoid of specific structure except for a few poorly developed desmosomes. The basal face has afferent synapses typical of the acousticolateralis receptors like in hair cells (see Hama, 1965, 1969). The presynaptic cytoplasm contains electron-dense bodies about 600 nm in diameter, surrounded by the synaptic vesicles (Fig. 2, *D* and *E*). A given nerve terminal in a synaptic area may be surrounded by 10 or more dense bodies. Mitochondria are present throughout the cytoplasm, particularly beneath the nucleus. Postsynaptically to the receptor cells, the myelinated afferent nerve fibers run along the duct, and are split several times over the ampulla. The final branches shed the myelin sheath as they penetrate the basement membrane and make the synaptic contacts with the receptor cells (Fig. 2 *B*). The nerve terminals contain abundant glycogen particles and mitochondria, as well as other membraneous structures (Fig. 2 *D*).

The supporting cells have basally located nuclei. The cytoplasm has abundant mitochondria and endoplasmic reticuli, and a few fatty bodies. Numerous small vesicles are also observed near the apical border of the thin processes (Fig. 2, *A* and *C*), which may be related to secretion of the ampullary jelly in the lumen (see Okitsu et al., 1978).

The duct wall is 2–6 μm thick, and consists of an epithelium of two or three cell layers. The adjacent epithelial cells within and between layers are loosely connected with desmosomes, and the tight junctional complexes are observed only at apposition among the cells in the most luminal layer. Interdigitated junctional complexes, such as in skate receptors (Waltman, 1966), have been rarely observed. The poorly developed junctional complex contrasts with the observation of extremely long space constant, which would suggest little leakage across the duct wall. The epithelium is separated by a basement membrane from many laminae of regularly oriented collagen fibers, which are three to four times thicker than the epithelium.

Physiology

Passive electrical properties of the ampulla. The electrically isolated ampulla showed a lumen-negative DC potential of 19.2 ± 6.5 mV (mean ± SD, n = 18) that

ranged from −10 to −37 mV, in contrast to the near zero DC potential in situ. The discrepancy has been ascribed to a steady bias current flow in the duct in situ (Sugawara and Obara, 1984*b*). The DC potential in the electrically isolated ampulla was insensitive to large changes in K^+ outside, which suggested involvement of ionic pumps at the basal membrane (Sugawara, 1986).

Fig. 3 *A* shows typical responses of the ampulla under the *I*-clamp. Large lumen-

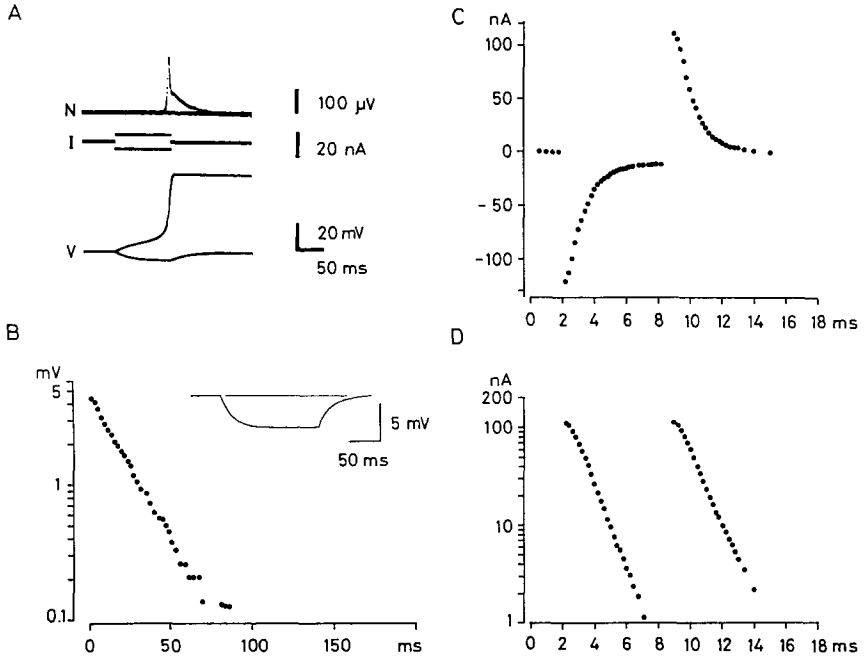

FIGURE 3. Passive properties of the sensory epithelium in standard saline. In *A*, typical responses under *I*-clamp are shown superimposed; with traces for externally recorded PSP (*N*) from the nerve in the presence of TTX, for stimulus current pulse (*I*), and for potential in the ampulla (*V*). Lumen-negative pulse evoked a negative electrotonic response while lumen-positive pulse of the same intensity provoked a regenerative response in the ampulla and PSP in the nerve. The DC-potential was −20 mV. In *B–D*, passive properties were compared in another ampulla. In *B* under *I*-clamp, a semilogarithmic plot of the negative response is shown against time after stimulus onset. The decay time constant was 20.8 ms, indicating a capacitance of 0.027 μF in parallel to an input resistance of 767 KΩ. In *C*, with the same ampulla under *V*-clamp, the current record on command step of −5.2 mV is shown, plotted only for the component after the initial 300 μs. In *D*, a semilogarithmic plot is fitted by a single exponential with the time constant of 1.3 ms. Total charge transfer is estimated as 0.13 nC, indicating that most part of the above capacitance, 0.025 μF, is in series to 52 KΩ.

positive stimulus evoked a regenerative response in the ampulla with prolonged PSP in the nerve. Lumen-negative stimulus evoked an electrotonic response. Passive properties were compared in another ampulla. In *B*, the voltage change under the *I*-clamp is shown in semilogarithmic plot to reveal an exponential decay with a time constant of 20.8 ms. The input resistance was 767 KΩ (697 ± 263 KΩ, $n = 21$), with

a range of 430–1,400 KΩ, and hence the capacitance was 0.027 μF (0.032 ± 0.01 μF, $n = 8$).

The same ampulla was next voltage-clamped at the resting DC level. Small voltage steps induced transient currents that were symmetrical for opposite polarities, and lasted for 2–3 ms (Fig. 3 *C*). The transient consisted of a few phases. The initial phase of ~300 μs followed the voltage steps. The second phase, however, declined exponentially in the face of a steady voltage level (Fig. 3 *D*), which suggested a part of the capacitance to be in series to a resistance. Integration of this phase indicated a charge transfer of 0.13 nC with a peak current of 100 nA to the command step of 5.2 mV, which implied a capacitance of 0.025 μF in series to 52 KΩ. Their product of 1.3 ms agreed well with the decay time constant (Fig. 3 *D*). Mean values of capacitance (0.022 ± 0.006 μF, $n = 14$) and time constant (1.116 ± 0.331 ms, $n = 16$) gave a series resistance of 50.7 KΩ, and a transepithelial capacitance of 0.01 μF.

The capacities thus measured may result from various sources. A major source, however, appears to be the basal (or basolateral) membrane of the receptor cells. As shown in the Morphology section, the receptor cells have the apical border demarcated by tight junctions. Assuming a cylinder 25 μm long and 15 μm across after fixation, the basal membrane area would be 0.0000135 cm^2 per cell. Surface area of the ampulla 300 μm in diameter is 0.0026 cm^2, excluding the exit of the duct. If this area were fully occupied by the receptor cells, the cell number would be ~1,500, making the total basal membrane area ~0.0203 cm^2. Assuming a specific membrane capacitance of 1 μF/cm^2, the total capacitance of single ampulla would be ~0.0203 μF. The receptor cells, however, are interspersed with the thin processes of the supporting cells (see Fig. 1 *A*), which may reduce the receptor cells to 700–1,000 per ampulla. The total basal area would then be 0.0095–0.0135 cm^2, making the capacitance 0.01–0.014 μF. These values, however, are probably an underestimate, considering a possible shrinkage during fixation.

The apical membrane area, and hence capacitance, is one order below the basal membrane area. If one attributes the series resistance of 50 KΩ to the apical membrane, the apical time constant would be <0.1 ms. This is two orders below 14 ms for the basal membrane. Hence, the apical capacitance may be ignored in *V*-clamp. The contribution of the supporting cell is difficult to estimate. Although their basal membrane area equals the surface area of the ampulla, their thin apical processes would give a large series resistance to the basal capacitance. A small, much slower current has been occasionally observed to follow the capacitative transient, which may represent the current through this current path.

Receptor Currents and Their Origin

Lumen-negative voltage steps induced ionic currents that were linear with voltages up to −150 mV. Lumen-positive steps induced nonlinear currents, associated with PSPs in the nerve (Fig. 4). As the nonlinear currents are ascribable to an inward current in the basal membrane of receptor cells, they will be shown as downward deflections. The inward currents were TTX-insensitive, and showed two components, i.e., an early transient with a peak at 5–7 ms and a delayed component with a peak at ~50 ms (Fig. 4 *A*). PSPs in the nerve also showed two components, with an initial PSP peak and a sustained PSP component (Fig. 4 *B*, left).

The current-voltage relations of both inward components were N-shaped and almost identical, with the maximum slope resistance of ~100 KΩ (Fig. 4 *C*). They reversed the sign also at the same voltage. The apparent reversal potential, however, was +34 mV, which was significantly lower than the PSP suppression potential (see Fig. 10). When Cd^{2+} (1 mM) was added to saline, the inward currents and PSPs were completely abolished (Fig. 4 *B*). The current-voltage relation became linear with a slope identical to the leakage resistance (Fig. 4 *C*). These data indicate that both

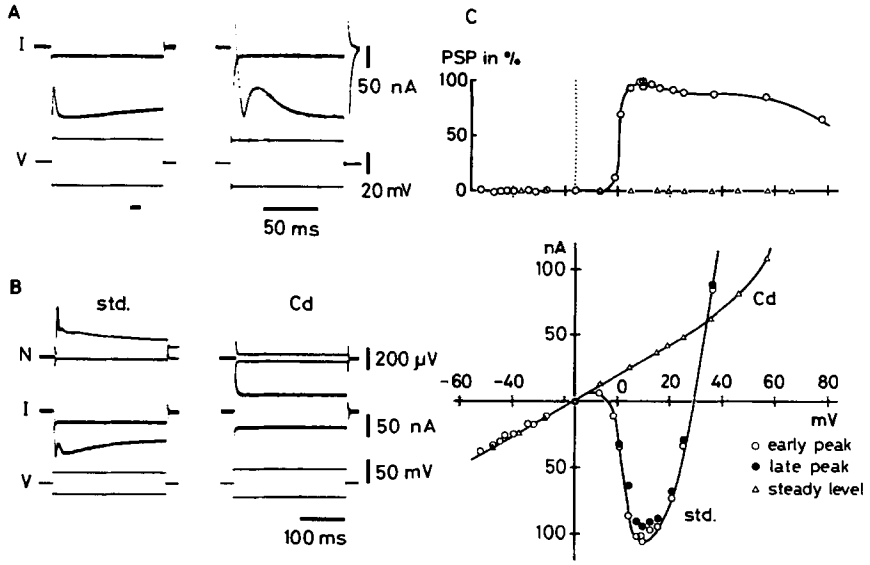

FIGURE 4. Epithelial current under *V*-clamp. *A* shows the current record in standard saline; with traces for the current (*I*), inward to the basal face of the receptor cells shown downward, and for the ampullary potential (*V*). Two responses on opposite command steps were superimposed, with records to the right on an expanded sweep to show the fast part. The lumen-negative step induced a leakage current after the capacitative surge. The lumen-positive step induced two inward current peaks. The holding potential was −17 mV. In *B*, both inward currents (*I*) and PSPs (*N*) were blocked by Cd^{2+} (1 mM) in another ampulla. The holding potential was −16 mV. In *C*, the current-voltage relation (lower panel) and PSP (upper panel) were plotted against the potential in the ampulla; for the early current peak, for PSP peak (open circles), and for the late current peak (closed circles) in saline. Both current peaks showed a similar N-shaped relation. Note that PSPs were not suppressed at voltage levels far beyond the reversal potential for the inward current. Cd^{2+} blocked all inward currents and PSPs, leaving the leakage currents (open triangles).

components are carried mainly by Ca^{2+} in the basal membrane of the receptor cells, which is accessible by Ca blockers outside the ampulla. This agrees well with the findings obtained in *I*-clamp (Akutsu and Obara, 1974). The low reversal potential, however, may indicate an involvement of outward currents.

The current pattern with the positive dip may suggest (*1*) an outward transient current superimposed over a maintained inward current, or (*2*) two populations of Ca channel, or both. Such outward transient may be further complicated, because

there are two membranes in series in the epithelium. Namely, the outward transient may represent either (*1a*) an inward current in the apical membrane as shown in skate (Clusin and Bennett, 1977*a*, *b*), or (*1b*) an actual outward current in the basal membrane. The present study has examined the first two possibilities *1a* and *1b*. A companion paper will discuss the presence of two populations of the Ca channel.

Absence of Apical Inward Current in the Plotosus Receptor

Lumen-positive stimuli hyperpolarize the apical membrane and depolarize the basal membrane, while lumen-negative stimuli have reverse effects. Either membrane

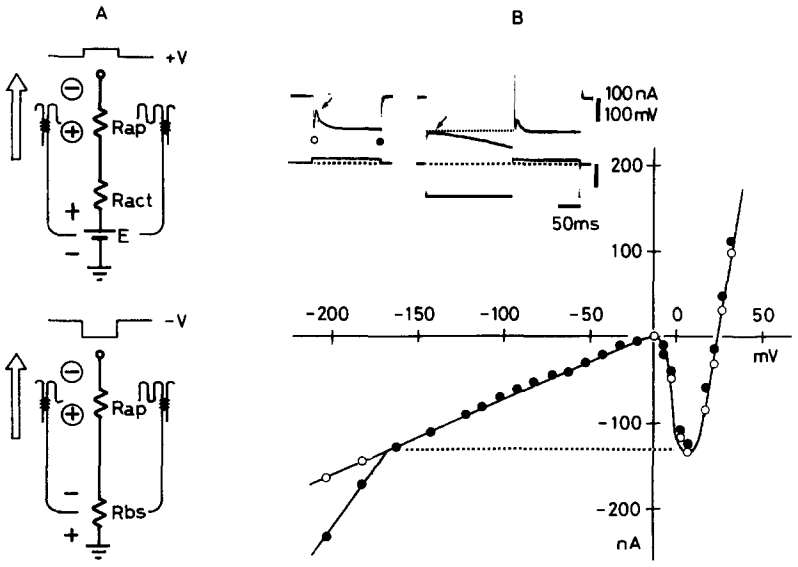

FIGURE 5. The "outward transient" is not due to an apical inward current. The diagram in *A* shows experimental protocol; with resistances (*R*ap and *R*bs) for the apical and basal faces of the receptor cell, and the active emf in the basal face (*E* with *R*act). The active emf (*E*) would supply depolarizing current to the apical face (upper diagram). Such depolarizing current may also be supplied by hyperpolarizing the whole epithelium (lower diagram). *B* shows the current-voltage relations for the early current peak (open circles) and for the current at the end of command steps (filled circles). Inset shows the sample records, with the control inward current shown to the left and with response for a large hyperpolarizing step to the right. The hyperpolarizing step evoked a gradually increasing inward current that would have supplied a depolarizing current to the apical face. No outward transient, however, was observed to mimic the control pattern (arrows in inset), even with the current as large as the maximum basal inward current (broken line in the graph). The holding potential was −16 mV.

thus depolarized may induce ionic currents. In skate receptors, the inward current induced in the apical membrane depolarizes the basal membrane sufficiently for transmitter secretion to the afferent nerve (Obara and Bennett, 1972; Clusin and Bennett, 1977*a*, *b*).

A reverse process, i.e., a basal inward current depolarizing the apical membrane to induce an apical inward current, would result in an apparent outward current.

This possibility was examined in Fig. 5. Large lumen-negative stimuli were given to depolarize the apical membrane. Pulses beyond −150 mV induced large slowly increasing currents that were close to the peak inward currents, but no positive dip was observed to mimic the inward current pattern (Fig. 5 *B*). The involvement of an apical activity thus appears unlikely in the *Plotosus* receptor.

Transient Outward Current in the Basal Membrane

The oscillatory response of the in situ ampulla is blocked by K blockers, which indicates involvement of K channels in the basal membrane (Sugawara and Obara,

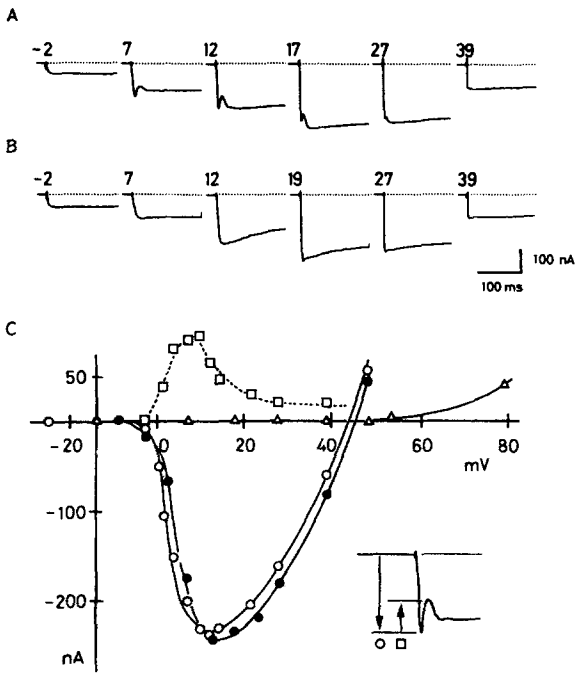

FIGURE 6. Suppression of the outward transient by 4-AP on the basal side. All current records are the net currents that are obtained by subtraction of the leakage currents. In *A*, the inward current in control saline showed two inward peaks with a positive dip. In *B*, the positive dip was nearly abolished by 4-AP (5 mM). In *C*, the current-voltage relations are plotted for the control early inward peak (open circles), for the peak current with 4-AP (closed circles), for the current after the addition of Cd^{2+} (open triangles), and for the outward transient (open squares). Amplitude of the outward transient was estimated as deviations of the positive dip from the inward current peak (inset). The outward transient was activated near the activation level for the inward current, and was suppressed beyond the reversal level for the latter. The leakage current gradually increased on steps over +60 mV, presumably due to the nonspecific conductance increase in the basal membrane. The holding potential was −13 mV.

1984*a*). The positive dip in the present current pattern may reflect the outward current in these channels. A series of net inward currents were obtained by subtracting leakage currents. The typical current pattern was seen in the mid-range (Fig. 6 *A*). 4-AP (5 mM/liter) completely abolished the positive dip (*B*). The addition of Cd^{2+} (0.5 mM/liter) abolished all nonlinear currents (*C*), even without prior 4-AP (see also Fig. 4 *B*).

In Fig. 6 *C*, the current-voltage relation was plotted for the net inward current. The outward transient was tentatively estimated as deviation of the positive dip from the peak inward current (see inset). The outward transient was induced at the activation level for the inward current, reached maximum near the voltage level for the

inward current maximum, and was suppressed beyond the apparent reversal level for the inward current. These results clearly indicate that the outward transient is caused by Ca-gated K current, $I_{K(Ca)}$, in the basal membrane.

The inward maximum current was barely increased by 4-AP (Fig. 6 *C*), which suggests little contamination of $I_{K(Ca)}$ to the peak inward current. The curve was sometimes shifted positively, but only by a few millivolts. The apparent reversal potential also remained nearly the same. Even after blockade by Cd^{2+}, a slowly increasing outward current was observed at voltages much higher than the apparent reversal potential, perhaps due to a nonspecific conductance increase upon excessive polarization.

Another test would be to replace Ca^{2+}, with Ba^{2+}, which is incapable of inducing the $I_{K(Ca)}$, although it carries ionic current in most Ca channels (Meech, 1978). Total substitution of Ca^{2+} with Ba^{2+} resulted in reversible abolition of the positive dip, again confirming the presence of $I_{K(Ca)}$.

Effects of Divalent Cations

The following experiments were carried out in the presence of K blockers. The net inward current showed biphasic decay from the peak (Fig. 7 *A*). When Ca^{2+} was increased from 3 to 10 mM/liter, the peak inward current increased and the initial decay became faster (*B*). The maximum current occurred at a more positive level, and the apparent reversal potential was shifted from +35 to +47 mV (*E*). On return to control saline, the inward current size was recovered completely, even though the current-voltage relation was shifted negatively by a few millivolts (*C* and *E*). In 1 mM/liter Ca^{2+}, the peak inward current decreased and the decay was retarded (*D*). The apparent reversal potential was shifted from +30 to +13 mV. Recovery from low Ca^{2+} concentration was incomplete, however, and was not included in the plot.

Thus, the current size and the reversal potential are both dependent on Ca concentration gradient across the basal membrane of receptor cells. The overall 34 mV/decade change, however, is probably an overestimate in view of the DC shift and the poor recovery after low Ca^{2+}. A more likely estimate of 22.9 mV/decade may be calculated on the basis of 12 mV change from 3 to 10 mM/liter Ca^{2+}, i.e., in a higher concentration range. This would suggest a less selective Ca^{2+} channel that permits outward currents.

The selectivity was further examined by ionic substitution. When Ca^{2+} was totally replaced by Ba^{2+}, the inward current decreased, and the apparent reversal potential shifted negatively (Fig. 8 *A*). Substitution with Sr^{2+} increased the inward current and the maximum slope. The apparent reversal potential, however, was shifted negatively (*B*). In both cases, recovery was relatively slow and incomplete. The shifts in reversal may be a less reliable measure for selectivity, because of possible contamination by the outward currents. Relative changes in the maximum current seem to suggest a selectivity in the order of $Sr^{2+} > Ca^{2+} > Ba^{2+}$.

Fig. 9 shows the effects of some ionic blockers. In the presence of K-blockers, the addition of Cd^{2+}, Mn^{2+}, or Mg^{2+} all suppressed the inward currents (*A* and *C*). Recovery was relatively poor, particularly with Cd^{2+}. The blocking effects are shown as normalized in Fig. 9 *C*. Curves are drawn by the following equation for the com-

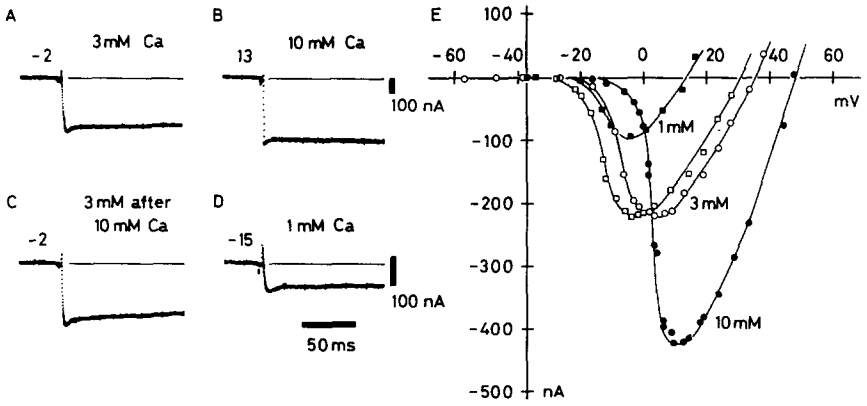

FIGURE 7. Effects of Ca^{2+} concentration change on the net inward current in the presence of 4-AP (5 mM) and TEA (20 mM). Sample records were shown for the maximum inward current; *A* in 3 mM Ca^{2+}, *B* in 10 mM, *C* recovery from 10 mM, and *D* in 1 mM. The command steps are marked on each record. Gain for all current records was the same except for *B*. In *E*, the current-voltage relations were plotted for the peak inward current; in 3 mM Ca^{2+} in control saline (open circles), in 10 mM (filled circles) on return to control saline (open squares), and in 1 mM (filled squares). Note the change in the inward current maxima and the shift in the apparent reversal levels. Recovery from low Ca concentration (1 mM) was incomplete, and not plotted. The holding potential was −37 mV.

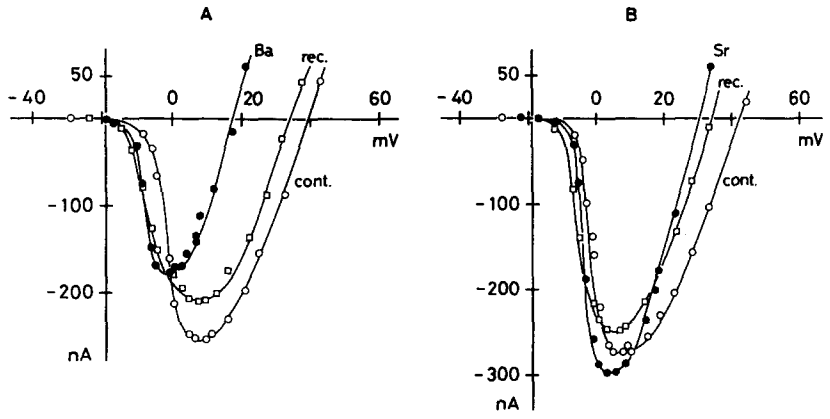

FIGURE 8. Inward currents induced in Ba and Sr saline in the presence of K blockers. Ca^{2+} in control saline was totally substituted with equimolar concentration of Ba^{2+} or Sr^{2+}. In *A*, the current-voltage relations are plotted for control currents in Ca saline (open circles), for currents in Ba saline (closed circles) and for those in recovery (open squares). In *B*, the current-voltage relations are for control Ca currents (open circles), for currents in Sr saline (filled circles) and for recovery (open squares). Recovery from Ba or Sr saline was slow and incomplete. The inward current maxima seem to suggest a selectivity in the order $Sr^{2+} > Ca^{2+} > Ba^{2+}$. The holding potential was −19 mV in *A* and −17 mV in *B*.

petitive inhibition (Hagiwara et al., 1974):

$$I_m/I_{Ca} = 1/(1 + [M]/K'_m) \quad (1)$$

where I_m represents the peak inward current in the presence of the blocker, I_{Ca} the control current, M the blocker, and K'_m the apparent dissociation constant for M, or $K'_m = K_m (1 + [Ca]/K_{Ca})$. The effects are similar to other Ca channels, and in the order of $Cd^{2+} > Mn^{2+} > Co^{2+} > Mg^{2+}$, with K'_m (in millimolar per liter): $K_{Mg} = 8.2$,

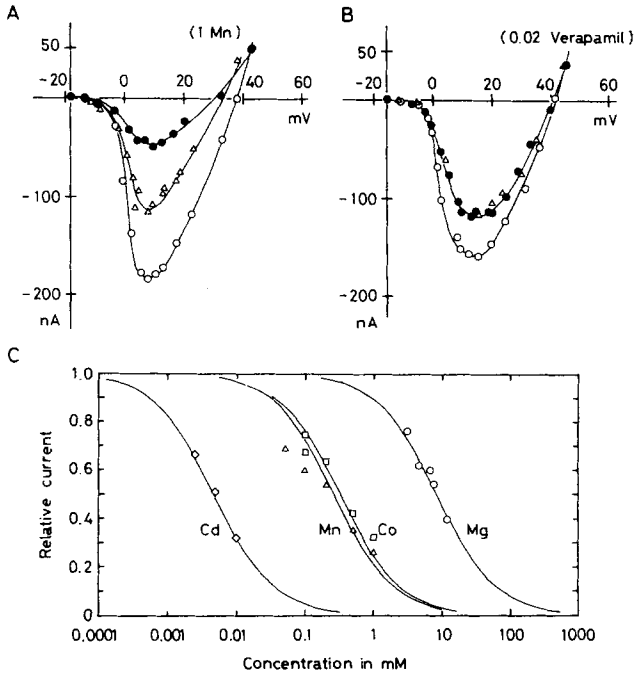

FIGURE 9. Block of the inward currents by divalent cations and verapamil in the presence of K blockers. Each blocker was added to control saline containing 3 mM/liter Ca^{2+}, except for Mg^{2+} which replaced Na^+ isosmotically. In the current-voltage relations the test saline contained 1 mM/liter Mn^{2+} in *A* and 0.02 mM/liter verapamil in *B*; open circles represent the peak inward currents in control saline, filled circles the currents in test saline, and open triangles the recovery. Recovery from the blockers was generally slow and incomplete, and the effect of verapamil was weak and irreversible. In *C*, the effects of divalent cations are shown normalized. Abscissa, log concentration of the blockers; ordinate, normalized currents. The curves are drawn by the equation, $I_m/I_{Ca} = 1/(1 + [M]/K'_m)$, with $K'_m = 4.7$ μM for Cd^{2+}, 0.26 mM for Mn^{2+}, 0.32 mM for Co^{2+}, and 8.2 mM for Mg^{2+}.

$K_{Co} = 0.32$, $K_{Mn} = 0.26$, and $K_{Cd} = 0.0047$. An organic blocker, verapamil, reduced the inward current by ~28% of the control at 20 μM/liter (Fig. 9 *B*). The effect was irreversible, and a further increase in dose simply failed to increase the effect.

Some Kinetic Aspects of the Inward Current

Despite limitations inherent in the voltage-clamp across an epithelium, the properties of the receptor Ca current were found to be similar to those of the Ca current in other excitable cells (see Hagiwara, 1983).

An inactivation process was examined by double-pulse experiments in the presence of K blocker. In Fig. 10 *A*, a conditioning pulse (P1) was stepped to +12 mV from the holding potential of −18 mV, and a test pulse (P2) to +10 mV at a 20-ms interval. The peak inward current to P2 was depressed by conditioning P1. Depression was dependent on the P1 level, and was maximum at +12 mV. Increasing P1

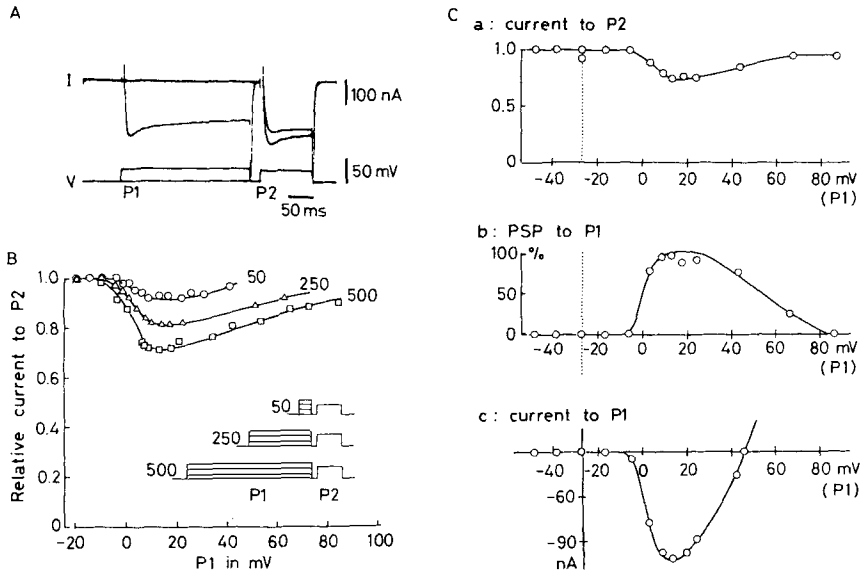

FIGURE 10. Current-dependent inactivation of the inward current in the presence of K blockers. The inset in *B* shows the protocol for double-pulse experiments. The test pulse (P2) of 100 ms in duration was stepped to +10 mV from the holding potential of −18 mV. The conditioning pulse (P1) preceded the test pulse by an interval of 20 ms. In *A*, the peak inward current to test P2 was clearly suppressed by conditioning P1 of +12 mV. In *B*, the peak inward currents to P2 are plotted against P1 of various durations: for 50 ms (open circles), for 250 ms (open triangles), and for 500 ms (open squares). The inward current was maximally suppressed around +12 mV, but recovered upon further P1 increase. The suppression became maximal with an increase in P1 duration to 500 ms, but it only rose to 70%. In *C*, suppression of the current to test P2 is shown to occur in a mirror image to PSP to conditioning P1 in another ampulla. The holding potential was −27 mV. P1 (500 ms) and P2 (100 ms) were given at 20-ms intervals. In *a*, the current to test P2 is similarly plotted against conditioning P1. In *b* and *c*, PSP and the current are both plotted to conditioning P1. Note that both the maximum suppression of current to P2 (*a*) and the maximum PSP to P1 (*b*) occur at voltage levels for the inward current maximum to P1 (*c*), and also that the suppression of current (*a*) is restored as P1 is further increased to over +85 mV beyond the PSP suppression potential (*b*).

further, however, resulted in a recovery (*B*). With an increase in P1 duration from 50 to 500 ms, depression of the current to test P2 became more pronounced, but only to ~70%. Such a mode of depression indicates that >30% of the peak current is inactivated in a current-dependent fashion. The steady current was less inactivated (Fig. 10 *A*), which is consistent with the observation of *I*-clamp that the receptor potential often persists over 5 min (see Fig. 3 *A*).

Voltage responses in the ampulla are closely related to the afferent activity via transmitter release (Obara, 1974; Obara and Sugawara, 1979). The mode of inactivation was therefore examined in reference to the PSP to P1. The input-output relation for peak postsynaptic potentials (PSP) to conditioning P1 (Fig. 10 *C*, *b*) showed a maximum at the level for the current maximum to P1 (*c*), and a suppression on further P1 increase over +85 mV. The inward current used to test P2 changed in a mirror image to PSP, with a maximum depression for the PSP maximum and a recovery for the PSP suppression (*a*). Assuming that the PSP amplitude is proportional to presynaptic Ca influx, and the PSP suppression potential represents the E_{Ca} (Katz and Miledi, 1969; Kusano, 1970), such a mode of depression for the current should indicate current-dependent inactivation. The PSP suppression potential ranged from +80 to +120 mV, and was always higher than the reversal potential, which also suggested a contamination of outward currents in the observed inward current.

DISCUSSION

The *Plotosus* receptors resemble the ampullae of Lorenzini of skate in their general organization of long radiating ducts, which are presumably useful for their adaptation to the high-conductance milieu of sea water common to both species. The teleost ampullae of *Plotosus*, however, are simple spheres, and are not lobulated as in skate. The receptor cells show fine structures similar to those of the fresh-water catfish. Such differences in structure have been correlated with the excitation polarity (see Bullock, 1982).

Space Clamp Conditions Across the Sensory Epithelium

The simple structure of the *Plotosus* ampullae seems to permit a fairly good spatial control. Rough estimates will be given below.

The input resistance is >700 KΩ, or 100 KΩ when active. Specific epithelial resistance would be 1.82 KΩ · cm^2 in the resting ampulla of 300 μm in diameter, or with an area of 0.0026 cm^2. Specific resistance of the jelly can be assumed to be similar to that of sea water, 25 Ω · cm. The ampulla may be replaced by a cylinder 170 μm in diameter, which is the same as that of the duct, with a closed end at 0.44 mm. In an infinite cable, space constant is 5.6 mm, and voltage drops to 92.4% at 0.44 mm. The cable, however, is terminated by an epithelium patch, and hence is nearly open-circuited with the voltage dropping to 99.7% at the termination. Thus, voltage in the ampulla would be fairly uniform. Even when active, a worst case assumption, a space constant of 2.1 mm and a voltage drop to 98% are expected. These estimates would ensure a good space clamp over the whole epithelium for DC.

The inactive apical membrane would act as a resistance of 50 KΩ in series to the basal membrane of 650 KΩ. The series resistance delays control of the basal membrane voltage by 2–3 ms during the capacitative surge, which would retard activation. With the fastest peak at 5–7 ms, however, the current record should be little affected. Conversely, axial resistance increase at the air gap induced a clear clamp failure.

The possibility remains that individual receptor cells may still escape because of the series resistance. Such escape was implied by low-amplitude graded oscillations

in the epithelial current to smaller command pulses in skate ampullae (Clusin and Bennett, 1977*b*). No oscillations, however, have been observed so far in the *Plotosus* ampullae.

Characterization of the Receptor Currents

The effects of the ionic blocker directly point to the basal membrane activity. In Fig. 10 *C* (*c*), the receptor current changes over a voltage span that is similar to other Ca current (Hagiwara, 1983). The PSP vs. P1 curve (*b*) is also similar to that intracellularly determined (cf. Kusano, 1970). Thus, even though the resting potential of receptor cells is unknown, the curves seem to represent those on the basal membrane, except with a DC shift.

The receptor current consists of the Ca current, I_{Ca}, and the Ca-gated transient K current, $I_{K(Ca)}$. The receptor I_{Ca} is similar to that described in various cells (Hagiwara

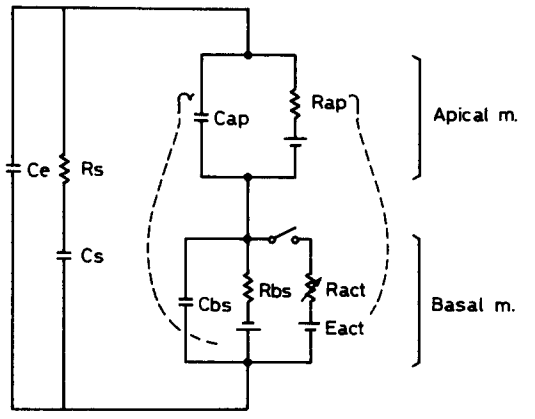

FIGURE 11. Equivalent circuit for the sensory epithelium of the *Plotosus* receptor. The receptor cells (700–1,000 per ampulla) are interspersed by the thin apical processes of the supporting cells. The following values are tentatively given per ampulla. The apical membrane (*Apical m.*) of the receptor cells are inactive, and are represented by *R*ap (50 KΩ) in parallel to *C*ap (0.002 μF). The basal membrane (*Basal m.*) is represented by *R*bs (650 KΩ) in parallel to *C*bs (0.022 μF), and in addition, by the active path with variable *R*act (50 KΩ) in series to *E*act that consists of Ca and K channels. The resting emf of both membranes are shown, but not labeled. A transepithelial capacitance is labeled as *C*e (0.01 μF). A much smaller current may also flow through complex configuration of the supporting cells that is represented by *C*s in series to *R*s.

and Byerly, 1981). It can be carried by Sr^{2+} or Ba^{2+}, and is blocked by divalent cations with efficacies similar to those in *Helix* neurons (Kostyuk et al., 1977; Akaike et al., 1978; Byerly et al., 1985). Verapamil is a potent Ca-blocker in cardiac and smooth muscles (Fleckenstein, 1977; Lee and Tsien, 1983). It is, however, less potent and only exerts an irreversible effect in the *Plotosus* receptor.

Under *I*-clamp, the receptor potential of *Plotosus* is regenerative and long lasting (Fig. 3), which has suggested a non-inactivating I_{Ca} (Akutsu and Obara, 1974). Under *V*-clamp, however, the receptor current gradually declines, even after $I_{K(Ca)}$ is completely blocked. A voltage-dependent inactivation can be excluded. The peak I_{Ca} is clearly inactivated in a current-dependent fashion, as shown in *Paramecium* (Brehm and Eckert, 1978; Brehm et al., 1980), in molluscan neurons (Tillotson, 1979; Eckert and Tillotson, 1981; Plant and Standen, 1981), in insect muscle (Ashcroft and Stanfield, 1981), and in frog heart (Mentrard et al., 1984). It has been claimed that Ca depletion in a narrow extracellular space causes a gradual decline of

I_{Ca} in frog muscle (Almers et al., 1981) and in *Neanthes* eggs (Fox and Krasne, 1984). In the *Plotosus* receptor, similar Ca depletion may well occur in the intercellular space around the receptor cell (see Fig. 2 *A*). Such a mechanism, however, would hardly account for the decline of receptor current. An increase in Ca concentration accelerates the current decline in *Plotosus* (Fig. 7), in contrast to deceleration as demonstrated in *Neanthes* eggs.

The receptor I_{Ca} reverses sign at 30–60 mV, which is significantly below the PSP suppression potential of 80–120 mV (Fig. 10). The discrepancy may be explained by an overestimation of the PSP suppression potential due to voltage drop at the apical membrane. The voltage drop, however, would amount to 10 mV at most, because the maximum current was <200 nA over the apical resistance of 50 KΩ. The lower reversal potential, or the clear reversal per se, suggests a Ca channel with nonspecific outward currents. Such Ca channels have been described in *Helix* neuron (Brown et al., 1981), in *Limnea* neuron (Byerly and Hagiwara, 1982), in chromaffin cell (Fenwick et al., 1982), in heart cell (Lee and Tsien, 1982), and in lymphocyte (Fukushima and Hagiwara, 1985). Their reversal potential is below +70 mV, close to the present data.

Operation of the Receptor Currents in Electroreception

In the acousticolateralis receptor, the apical and basal membranes of the receptor cells serve for different functions. Voltage clamp on the sensory epithelium can differentiate these activities. As the electroreceptors detect voltage changes across the epithelium, either membrane may serve for transduction. Two strategies apparently have evolved.

In nonteleost receptors, the apical membrane serves for transduction, while the basal membrane for secretion, presynaptic to the afferent nerve. In the ampullae of Lorenzini, the apical membrane shows noninactivating Ca current followed by Ca-gated and maintained K current. The basal membrane has small Ca and K currents which, though primarily involved in secretion, may also contribute to receptor responses. Under in situ conditions, the apical membrane is tonically active, generating a train of receptor spikes that depolarize the basal membrane for secretion. Full-sized receptor spikes, asynchronous among individual cells, are implied by oscillations in current and in PSP (Clusin and Bennett, 1977*a*, *b*; 1979*a*, *b*).

In teleost receptors, the basal membrane serves for both transduction and secretion, while the apical membrane provides either a low-impedance access or a signal filtering to the receptor activity (see Bennett, 1971). The tonic, teleost ampullae of *Plotosus* have Ca current and Ca-gated K current, but in the basal membrane and with different channel properties. Under in situ conditions, the basal membrane is clearly held depolarized and partially activated for secretion. The receptor activity, however, seems to be graded, since no oscillations such as those found in skate receptors have been observed (Sugawara and Obara, 1984*a*, *b*).

The receptor operation therefore, differs a great deal between the two species. In nonteleost receptors, signals on the epithelium would be best detected if the basal membrane resistance were small so that the apical membrane could receive most of the signals. The basal membrane resistance, however, must be large enough for the apical inward current to depolarize for secretion. The receptor spike may be a com-

promise for such conflicting requirements. In teleost receptors, both transduction and secretion occur in the same membrane, which obviates such problems. The graded receptor activity then might suffice. Intracellular study is required for direct comparison.

Roles of Ca Ions in the Acousticolateralis Receptors

The cochlear transduction hypothesis is based on the K-rich endolymph and the positive endocochlear DC potential (Davis, 1965). A similarly K-rich microenvironment has been shown in the apical cupula in the free neuromasts of *Xenopus* (Russell and Sellick, 1976).

The transduction channels are located in the apical membrane (Hudspeth and Jacobs, 1979; Hudspeth, 1982). They are relatively nonselective for monovalent cations, Li^+, Na^+, K^+, Cs^+, or even TEA^+ as shown in frog (Corey and Hudspeth, 1979) and in chick (Ohmori, 1985), though under physiological conditions the transduction current is perhaps carried by K^+. They are also permeable to divalent cations, and are blocked by Ca-blockers such as Co^{2+}, La^{3+}, and other organic blockers (Ohmori, 1985).

The role of Ca^{2+} in transduction remains unclear. In the lateral-line organ of mudpuppy, the mechano-sensitivity does increase as a function of Ca concentration (Sand, 1975). The ionized Ca^{2+} in cupula is only 2–30 μM in *Xenopus* (McGlone et al., 1979) and 30 μM in the endolymph (Bosher and Warren, 1978). Nevertheless, the transduction current fails at 10 μM Ca^{2+} in frog (Corey and Hudspeth, 1979), or requires at least 20 μM Ca^{2+} in Cs saline in chick (Ohmori, 1985).

The hair cells also have Ca current and various K currents, probably in the basal membrane (Lewis and Hudspeth, 1983; Ohmori, 1984*a*, *b*; Hudspeth, 1985). Depolarizing current steps induce damped voltage oscillations in the frog hair cell, which are ascribed to a non-inactivating Ca current and a Ca-gated K current. In turtle, electrically induced oscillations show a best frequency in each cell that is identical to the best frequency of the intracellular microphonic potential (Crawford and Fettiplace, 1981). Thus, at least in lower vertebrates, the Ca channel in the basal membrane seems to serve for electrical tuning in transduction. The afferent nerves in some electroreceptor are tuned as sharply as that of the hair cells (Hopkins, 1976), and similar ionic mechanisms for electrical tuning have been recently suggested (Zakon, 1984).

The authors are indebted to Dr. Toku Kanaseki, Tokyo Metropolitan Institute for Neurosciences, Fuchu-City Tokyo, for his guidance and helpful advice in the anatomical study.

This work was supported in part by the grant from the Ministry of Education, Science and Culture of Japan, 548101.

Original version received 3 June 1987 and accepted version received 7 September 1988.

REFERENCES

Akaike, N., K. Lee, and A. M. Brown. 1978. The calcium current of *Helix* neuron. *Journal of General Physiology.* 71:509–531.

Akutsu, Y., and S. Obara. 1974. Calcium dependent receptor potential of the electroreceptor of marine catfish. *Proceedings of the Japan Academy.* 50:247–251.

Almers, W., R. Fink, and P. T. Palade. 1981. Calcium depletion in frog muscle tubules: the decline of calcium current under maintained depolarization. *Journal of Physiology.* 312:177–207.

Ashcroft, F. M., and P. R. Stanfield. 1981. Calcium dependence of the inactivation of calcium currents in skeletal muscle fibers of an insect. *Science.* 213:224–226.

Bennett, M. V. L. 1971. Electroreception. *In* Fish Physiology. Vol. 5. W. S. Hoar and D. J. Randall, editors. Academic Press, Inc. New York. 493–574.

Bosher, S. K., and R. L. Warren. 1978. Very low calcium content of cochlear endolymph, an extracellular fluid. *Nature.* 273:377–378.

Brehm, P., and R. Eckert. 1978. Calcium entry leads to inactivation of calcium channel in *Paramecium. Science.* 202:1203–1206.

Brehm, P., R. Eckert, and D. Tillottson. 1980. Calcium-mediated inactivation of calcium current in *Paramecium. Journal of Physiology.* 306:193–203.

Brown, A. M., K. Morimoto, Y. Tsuda, and D. L. Willson. 1981. Calcium current–dependent and voltage–dependent inactivation of calcium channels in *Helix aspersa. Journal of Physiology.* 320:193–218.

Bullock, T. H. 1982. Electroreception. *Annual Review of Neuroscience.* 5:121–170.

Byerly, L., P. B. Chase, and J. R. Stimers. 1985. Permeation and interaction of divalent cations in calcium channels of snail neurons. *Journal of General Physiology.* 85:491–518.

Byerly, L. and S. Hagiwara. 1982. Calcium currents in internally perfused nerve cell bodies of *Limnea stagnalis. Journal of Physiology.* 322:503–528.

Clusin, W. T., and M. V. L. Bennett. 1977*a*. Calcium-activated conductance in skate electroreceptors. Current clamp experiments. *Journal of General Physiology.* 69:121–143.

Clusin, W. T., and M. V. L. Bennett. 1977*b*. Calcium-activated conductance in skate electroreceptors. Voltage clamp experiments. *Journal of General Physiology.* 69:145–182.

Clusin, W. T., and M. V. L. Bennett. 1979*a*. The oscillatory responses of skate electroreceptors to small voltage stimuli. *Journal of General Physiology.* 73:685–702.

Clusin, W. T., and M. V. L. Bennett. 1979*b*. The ionic basis of oscillatory responses of skate receptors. *Journal of General Physiology.* 73:703–723.

Corey, D. P., and A. J. Hudspeth. 1979. Ionic basis of the receptor potential in a vertebrate hair cell. *Nature.* 281:675–677.

Crawford, A. C., and R. Fettiplace. 1981. An electrical tuning mechanism in turtle cochlear hair cells. *Journal of Physiology.* 312:377–412.

Davis, H. 1965. A model for transducer action in the cochlea. *Cold Spring Harbor Symposium of Quantitative Biology.* 30:181–190.

Eckert, R., and D. L. Tillotson. 1981. Calcium-mediated inactivation of the calcium conductance in caesium-loaded giant neurones of *Aplysia californica. Journal of Physiology.* 314:265–280.

Fain, G. L., F. N. Quandt, and H. M. Gerschenfeld. 1977. Calcium-dependent regenerative responses in rods. *Nature.* 269:707–710.

Fenwick, E. M., A. Marty, and E. Neher. 1982. Sodium and calcium channels in bovine chromaffin cells. *Journal of Physiology.* 331:599–635.

Fleckenstein, A. 1977. Specific pharmacology of calcium in myocardium, cardiac pacemakers, and vascular smooth muscle. *Annual Review of Pharmacology and Toxicology.* 17:149–166.

Fox, A. P., and S. Krasne. 1984. Two calcium currents in *Neanthes arenaceodentatus* egg cell membranes. *Journal of Physiology.* 356:491–505.

Friedrich-Freksa, H. 1930. Lorenzinische Ampullen bei dem Siluroiden *Plotosus anguillaris* Bloch. *Zoologischer Anzeiger.* 87:49–66.

Fukushima, Y., and S. Hagiwara. 1985. Current carried by monovalent cations through calcium channels in mouse neoplastic B lymphocytes. *Journal of Physiology.* 358:255–284.

Hagiwara, S. 1983. Membrane potential-dependent ion channels in cell membrane. *In* Distinguished Lecture Series of the Society of General Physiologists. Vol. 3. Raven Press, New York. 5–33.

Hagiwara, S., and L. Byerly. 1981. Calcium channel. *Annual Review of Neuroscience.* 4:69–125.

Hagiwara, S., J. Fukuda, and D. Eaton. 1974. Membrane currents carried by Ca, Sr, and Ba in barnacle muscle fiber during voltage clamp. *Journal of General Physiology.* 63:564–578.

Hama, K. 1965. Some observations on the fine structure of the lateral line organ of the Japanese sea eel (*Lyncozymba nystromi*). *Journal of Cell Biology.* 24:193–210.

Hama, K. 1969. A study on the fine structure of the saccular macula of the gold fish. *Zeitschrift für Zellforschung und Mikroskopische Anatomie.* 94:155–171.

Hopkins, C. D. 1976. Stimulus filtering and electroreception: tuberous electroreceptors in three species of Gymnotoid fish. *Journal of Comparative Physiology.* 111:171–207.

Hudspeth, A. J. 1982. Extracellular current flow and the site of transduction by vestibular hair cells. *Journal of Neuroscience.* 2:1–10.

Hudspeth, A. J. 1985. The cellular basis of hearing: the biophysics of hair cells. *Science.* 230:745–752.

Hudspeth, A. J., and R. Jacobs. 1979. Stereocilia mediate transduction in vertebrate hair cells. *Proceedings of the National Academy of Sciences.* 76:1506–1509.

Katz, B., and R. Miledi. 1969. Tetrodotoxin resistant electric activity in presynaptic terminals. *Journal of Physiology.* 203:459–489.

Kostyuk, P. G., O. A. Krishtal, and Y. A. Shakhovalov. 1977. Separation of sodium and calcium currents in the somatic membrane of mollusc neurones. *Journal of Physiology.* 270:545–568.

Kusano, K. 1970. Influence of ionic environment on the relationship between pre- and postsynaptic potentials. *Journal of Neurobiology.* 1:435–457.

Lee, K. S., and R. W. Tsien. 1982. Reversal of current through calcium channels in dialysis single heart cells. *Nature.* 297:498–501.

Lee, K. S., and R. W. Tsien. 1983. Mechanism of calcium channel blockade by verapamil, D600, diltiazem and nitrendipine in single dialysed heart cells. *Nature.* 302:790–794.

Lekander, B. 1949. The sensory line system and the canal bones in the head of some Ostariophysi. *Acta Zoologica.* 30:1–131.

Lewis, R. S., and A. J. Hudspeth. 1983. Voltage- and ion-dependent conductances in solitary vertebrate hair cells. *Nature.* 304:538–541.

Lissmann, H. W., and A. M. Mullinger. 1968. Organization of ampullary electric receptors in Gymnotidae (Pisces). *Proceedings of the Royal Society of London, Series B.* 169:345–378.

McGlone, F. P., I. J. Russell, and O. Sand. 1979. Measurement of calcium ion concentrations in the lateral line cupulae of *Xenopus laevis*. *Journal of Experimental Biology.* 83:123–130.

Meech, R. W. 1978. Calcium dependent potassium activation in nervous tissues. *Annual Review of Biophysics and Bioengineering.* 7:1–18.

Mentrard, D., G. Vassort, and R. Fischmeister. 1984. Calcium-mediated inactivation of the calcium conductance in cesium-loaded frog heart cells. *Journal of General Physiology.* 83:105–131.

Naitoh, Y., and R. Eckert. 1969. Ionic mechanisms controlling behavioral responses of paramecium to mechanical stimulation. *Science.* 164:963–965.

Obara, S. 1974. Receptor cell activity at "rest" with respect to the tonic operation of a specialized lateralis receptor. *Proceedings of the Japan Academy.* 50:386–391.

Obara, S., and M. V. L. Bennett. 1972. Mode of operation of ampullae of Lorenzini of skate, *Raja*. *Journal of General Physiology.* 60:534–557.

Obara, S., and Y. Sugawara. 1979. Contribution of Ca to electroreceptor mechanism in *Plotosus* ampullae. *Journal de Physiologie.* 75:335–340.

Ohmori, H. 1984*a*. Mechanoelectrical transducer has discrete conductances in the chick vestibular hair cell. *Proceedings of the National Academy of Sciences.* 81:1888–1891.

Ohmori, H. 1984*b*. Studies of ionic currents in the isolated vestibular hair cell of the chick. *Journal of Physiology.* 350:561–581.

Ohmori, H. 1985. Mechano-electrical transduction currents in isolated vestibular hair cells of the chick. *Journal of Physiology.* 359:189–217.

Okitsu, S., S. Umekita, and S. Obara. 1978. Ionic compositions of the media across the sensory epithelium in the ampullae of Lorenzini of the marine catfish, *Plotosus. Journal of Comparative Physiology.* 126:115–121.

Plant, T. D., and N. B. Standen. 1981. Calcium current inactivation in identified neurones of *Helix aspersa. Journal of Physiology.* 321:273–285.

Ross, W. N., and A. E. Stuart. 1978. Voltage sensitive calcium channels in the presynaptic terminals of decrementally conducting photoreceptor. *Journal of Physiology.* 274:173–191.

Russell, I. J., and P. M. Sellick. 1976. Measurement of potassium and chloride ion concentrations in the cupulae of the lateral lines of *Xenopus laevis. Journal of Physiology.* 257:245–255.

Sand, O. 1975. Effects of different ionic environments on the mechano-sensitivity of lateral line organs in the mudpuppy. *Journal of Comparative Physiology, A.* 102:27–42.

Sugawara, Y. 1986. Contribution of ionic pumps to the DC potential and receptor activity of *Plotosus* electroreceptors. *Journal of the Physiological Society of Japan.* 48:305. (Abstr.)

Sugawara, Y., and T. Kanaseki. 1976. A combined physiological and electron microscope study of the electroreceptor of marine catfish, *Plotosus anguillaris* (*Lcépède*), with special reference to the mechanisms of afferent transmissions. *Journal of Electron Microscopy.* 25:214–215. (Abstr.)

Sugawara, Y., and S. Obara. 1979. Voltage-clamp analysis of the Ca dependent receptor potential in *Plotosus* electroreceptor. *Neuroscience Letters Supplement.* 2:S3. (Abstr.)

Sugawara, Y., and S. Obara. 1984*a*. Damped oscillation in the ampullary electroreceptors of *Plotosus* involves Ca-activated transient K conductance in the basal membrane of receptor cells. *Brain Research.* 302:171–175.

Sugawara, Y., and S. Obara. 1984*b*. Ionic currents in the sensory epithelium examined in isolated electroreceptors of *Plotosus* under simulated in situ conditions. *Brain Research.* 302:176–179.

Tillotson, D. 1979. Inactivation of Ca conductance is dependent on entry of Ca ions in molluscan neurones. *Proceedings of the National Academy of Sciences.* 76:1497–1500.

Waltman, B. 1966. Electrical properties and fine structure of the ampullary canals of Lorenzini. *Acta Physiological Scandinavica Supplement.* 264:5–60.

Zakon, H. H. 1984. Tuning of newly generated electroreceptors. *Neuroscience.* 10:193. (Abstr.)

Zipser, B., and M. V. L. Bennett. 1973. Tetrodotoxin resistant electrically excitable responses of receptor cells. *Brain Research.* 62:253–259.